Interrelationships between Conformational Dynamics and the Redox Chemistry of *S*-Nitrosothiols

N. Arulsamy,[†] D. S. Bohle,*[,†] J. A. Butt,[‡] G. J. Irvine,[†] P. A. Jordan,*[,†] and E. Sagan[†]

Contribution from the Department of Chemistry, University of Wyoming, Laramie, Wyoming 82071-3838, and Centre for Metalloprotein Spectroscopy and Biology, School of Chemical Sciences, University of East Anglia, Norwich NR4 7TJ, United Kingdom

Received January 13, 1999. Revised Manuscript Received May 12, 1999

Abstract: An increasing number of biological roles are ascribed to *S*-nitrosothiol compounds. Their inherent instability in multicomponent solutions is recognized as forming the basis for their physiological effects, such as the release of nitric oxide or the posttranslational modification of protein cysteine residues. This reactivity also contributes to the lack of fundamental physical and spectroscopic data that have been reported. We have addressed this issue through characterization of the physical and spectroscopic properties of a group of commonly used *S*-nitrosothiols. The *S*-nitrosothiol Ph_3CSNO, which is readily prepared by the biphasic nitrosation of Ph_3CSH, is characterized by X-ray diffraction, vibrational spectroscopy, electrochemistry, and spectroelectrochemistry. Its behavior is contrasted with that of known *S*-nitrosothiols derived from glutathione and *N*-acetyl-D,L-penicillamine, which also are demonstrated to undergo facile electrochemical and chemical denitrosylation. The structure and vibrational data are contrasted with ab initio results calculated with density functional theory, B3LYP/6-311+G*, which indicates that electron transfer populates an orbital that is strongly ON−SR antibonding in character. The bond lengths observed for Ph_3CSNO (N−O 1.18 Å, S−N 1.79 Å) indicate a formal nitrogen-to-oxygen double bond and sulfur−oxygen single bond. However, theoretical calculations show a measure of delocalization over the −CSNO framework. This is supported by experimental results that show low ν(NO) vibrational frequencies (1470−1515 cm^{-1}) and a large $\Delta G^{\ddagger}$ (10.7 kcal/mol) for syn−anti interconversion determined by variable-temperature ^{15}N NMR. Together these results demonstrate an important new reactivity pattern for this biologically critical class of compounds.

Introduction

The important disclosure that nitric oxide (NO) plays an essential regulatory role in physiological systems proved a watershed in terms of research.[1,2] In no time at all a plethora of investigations followed into the many different aspects of NO biochemistry: the generation of nitric oxide, its function, and fate.[3−8] As part of this extensive research the presence of *S*-nitrosothiols, RSNO, in biological systems was demonstrated.[9,10] This led to considerable interest into the physiological role of *S*-nitrosothiol species and their formation and reactivity, either as a small molecule adduct or as a posttranslational chemical modification to a protein. Previous studies have shown that in vitro proteins containing free cysteine residues can be readily converted to the corresponding Cys-SNO. This has been demonstrated for serum albumin (bovine and human), papain, and tissue plasminogen activator.[11,12] In an important set of recent papers a physiological role for *S*-nitrosothiols has been proposed.[13−15] From this work Stamler et al. propose that hemoglobin can act as both an oxygen and nitric oxide transporter. The premise is that deoxyhemoglobin scavenges nitric oxide in postcapillary vasculature, this is followed by NO group exchange from heme to Cys-β_{93} in the lung, with release of NO being triggered by allosteric changes in hemoglobin in response to low pO_2.

The observation of the *S*-nitrosothiol functional group is, however, not new. In a 1909 report Tasker and Jones observed that the unstable *S*-nitrosophenylthiol could be prepared from benzenethiol and nitrosyl chloride,[16] and in 1983, before the physiological role of nitric oxide was recognized, an excellent review was published concerning the nitrosation products of thiol groups in organic systems.[17] The formation of RSNO species from the reaction of nitrogen oxides with a wide range

[†] University of Wyoming.
[‡] University of East Anglia.

(1) *Nitric Oxide Part B: Physiological and Pathological processes*; Packer, L., Ed.; Academic Press: San Diego, 1996; Vol. 269.
(2) *Nitric Oxide Part A: Sources and Detection of NO; NO synthase*; Packer, L., Ed.; Academic Press: San Diego, 1996; Vol. 268.
(3) Marletta, M. A. *J. Biol. Chem.* **1993**, *268*, 12231−12234.
(4) Nathan, C.; Xie, Q. *J. Biol. Chem.* **1994**, *269*, 13725−13728.
(5) Crane, B. R.; Arvai, A. S.; Ghosh, D. K.; Wu, C.; Getzoff, E. D.; Steuhr, D. J.; Tainer, J. A. *Science* **1998**, *279*, 2121−2126.
(6) Bredt, D. S.; Snyder, S. H. *Annu. Rev. Biochem.* **1993**, *63*, 175−195.
(7) Gross, S. S.; Wolin, M. S. *Annu. Rev. Physiol.* **1995**, *57*, 737−769.
(8) Kerwin, J. F.; Lancaster, J. R.; Feldman, P. L. *J. Med. Chem.* **1995**, *38*, 4343−4362.
(9) Goldman, R. K.; Vlessis, A. A.; Trunkey, D. D. *Anal. Biochem.* **1998**, *259*, 98−103.
(10) Rockett, K. A.; Awburn, M. M.; Cowden, W. B.; Clark, I. A. *Infect. Immun.* **1991**, *59*, 3280−3283.
(11) Stamler, J. S.; Simon, D. I.; Osborne, J. A.; Mullins, M. E.; Jaraki, O.; Singel, D. J.; Loscalzo, J. *Proc. Natl. Acad. Sci. U.S.A.* **1992**, *89*, 444−448.
(12) Guo, Z. M.; Ramirez, J.; Li, J.; Wang, P. G. *J. Am. Chem. Soc.* **1998**, *120*, 3726−3734.
(13) Gow, A. J.; Stamler, J. S. *Nature* **1998**, *391*, 169−173.
(14) Jia, L.; Bonaventura, C.; Bonaventura, J.; Stamler, J. S. *Nature* **1996**, *380*, 221−226.
(15) Stamler, J. S.; Jia, L.; Eu, J. P.; McMahon, T. J.; Demchenko, I. T.; Bonaventura, J.; Gernert, K.; Piantadosi, C. A. *Science* **1997**, *276*, 2034−2037.
(16) Tasker, H. S.; Jones, H. O. *J. Chem. Soc.* **1909**, *95*, 1910−1918.
(17) Oae, S.; Shinhama, K. *Org. Prep. Proced. Int.* **1983**, *15*, 165−198.

10.1021/ja9901314 CCC: $18.00
Published on Web 07/16/1999

of thiols has been demonstrated spectroscopically. However, confusion remains in the literature surrounding the reactivity of the RSNO functional group, and in particular the factors affecting its decomposition.[18−23] In addition, there is only a single X-ray crystal structure available of an *S*-nitrosothiol, *S*-nitrosoacetyl-D,L-penicillamine (SNAP), in the Cambridge crystallographic database.[24] These factors demonstrate that a number of significant hurdles remain in the complete dissemination of the physiological role for RSNO species. Notable among these are suitable methods for the detection of and adequate structural details for the −SNO functional group. The inherent instability of the RSNO group poses a number of challenges for the isolation and characterization of these compounds. In recent years there have been advances in the detection of the decomposition products from *S*-nitrosothiols, using better coupling reagents as chromophores and fluorophores[25] or chemiluminescence.[26,27] However, a majority of studies still rely upon the venerable Saville method for the bulk determination of RSNO.[28] In this paper we report the following: (i) the X-ray crystal structure of Ph_3CSNO, (ii) ab initio ground-state geometry and frequencies for MeSNO and its $1e^-$ reduced form, (iii) variable-temperature ^{15}N NMR study of $(CH_3)_3CSNO$, (iv) vibrational spectroscopic results for the compounds GSNO, SNAP, and Ph_3CSNO, and (v) fundamental reactions of this class of compounds. The results substantiate the solid-state preference for the anti conformation of the R−S−N−O linkage, although the syn conformation is the theoretically determined minimum for CH_3SNO, and demonstrate that vibrations sensitive to the −SNO group can be detected by using both IR and Raman spectroscopy. Analysis of the patterns of decomposition for three different RSNO groups shows that these compounds are stable to oxidation but undergo rapid reductive elimination of the NO group. This is supported by theoretical calculations that show a lengthening of the S−N bond in the $MeSNO^{\bullet-}$ radical anion.

Results

Most syntheses of *S*-nitrosothiols in organic systems involve N_2O_4 and are hampered by preparation and handling of this reagent. Because N_2O_4 is a powerful oxidant it is not compatible with many substituents.[17,29] In principle the use of a two-phase system to prepare *S*-nitrosothiols will circumvent these problems, and surprisingly has not been reported previously. Through this method generation of *S*-nitrosotriphenylmethanethiol is straightforward, the thiol reacts rapidly with aqueous acidified sodium nitrite. The green product is readily precipitated upon addition of methanol to the organic layer and cooling to −10 °C. Needle-shaped crystals are isolated, at a lower yield, by adding less methanol. The solid is dark green when recovered but decomposes to a yellow product upon prolonged exposure to ordinary fluorescent light. It is also possible to prepare the *S*-nitroso-2-methyl-2-propanethiol, $(CH_3)_3CSNO$, with this method.

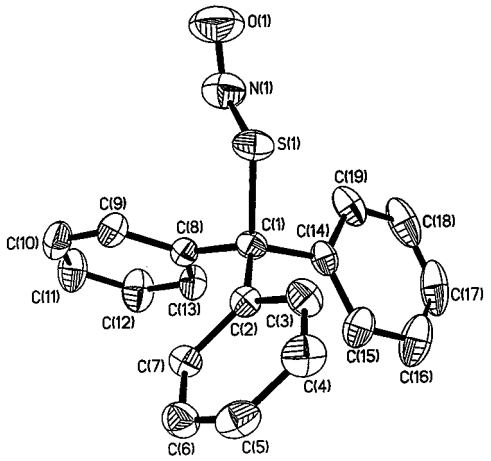

Figure 1. X-ray crystal structure for Ph_3CSNO.

Table 1. Structural Analysis Parameters

compd	Ph_3CSNO	SNAP
formula	$C_{19}H_{15}NOS$	$C_7H_{12}N_2O_4S$
crystal size, mm	0.12 × 0.48 × 1.20	0.76 × 0.52.0.40
space group	$Pna2_1$	$P2_12_12$
a, Å	7.4073(7)	12.173(2)
b, Å	28.165(3)	13.548(2)
c, Å	7.5793(10)	6.4940(10)
V, Å^3	1581.2(3)	1071.0(3)
$\alpha = \beta = \gamma$, deg	90	90
Z	4	4
temperature, °C	25	−100
no. of independent reflcns	1724	1409
data-to-parameter ratio	6.6:1	8:1
R^a	0.0415	0.0256
$R_w{}^a$	0.1143	0.0677

[a] $w^{-1} = \sigma^2F_o^2 + (0.0815P)^2 + 0.25P$, here $P = (F_o^2 + 2F_c^2)/3$.

Table 2. Selected Bond Lengths (Å) and Angles (deg) for Ph_3CSNO

bond	length, Å	bond	angle, deg
N−O	1.177(6)	O−N−S	114.0(4)
S−N	1.792(5)	N−S−C(1)	102.1(2)
C(1)−S	1.867(3)	C(2)−C(1)−C(8)	112.5(2)
C(1)−C(2)	1.532(4)	C(2)−C(1)−S	102.4
C(1)−C(8)	1.534(4)	C(1)−S(1)−N(1)−O(1)	175.7
C(1)−C(14)	1.533(4)		

The X-ray crystal structure of *S*-nitrosotriphenylmethanethiol is presented in Figure 1 and pertinent bond lengths and angles given in Table 2. The R−S−N═O linkage is bent approximating an anti conformation. The observed bond lengths (S−N 1.792(5) Å, N−O 1.177(6) Å) are consistent with a sulfur−nitrogen single bond and a nitrogen−oxygen double bond. The C−S−N−O framework is nearly planar, with the largest out-of-plane deviation being 0.0327 Å by N_1, and adopts an anti configuration with a C−S−N−O dihedral angle $\tau = 175.7°$. A comparison of this structure with (1) *S*-nitroso-D,L,-acetylpenicillamine, (2) the theoretically predicted ground-state structure of MeSNO, and (3) the $1e^-$ reduced form $\{MeSNO\}^-$ is given in Table 3. The structure of MeSNO is given in Figure 2 and the predicted vibrational modes in Figure 3. The bond lengths and angles associated with the CSNO group in Ph_3CSNO and SNAP are very similar showing the presence of the same

(18) Holmes, A. J.; Williams, D. L. H. *Chem. Commun.* **1998**, 1711−1712.
(19) Dicks, A. P.; Beloso, P. H.; Williams, D. L. H. *J. Chem. Soc., Perkin Trans. 2* **1997**, 1429−1434.
(20) Singh, S. P.; Wishnok, J. S.; Keshive, M.; Deen, W. M.; Tannenbaum, S. R. *Proc. Natl. Acad. Sci. U.S.A.* **1996**, *93*, 14428−14433.
(21) Singh, R. J.; Hogg, N.; Joseph, J.; Kalyanaraman, B. *J. Biol. Chem.* **1996**, *271*, 18596−18603.
(22) Arnelle, D. R.; Stamler, J. S. *Arch. Biochem. Biophys.* **1995**, *318*, 279−285.
(23) Arnelle, D. R.; Day, B. J.; Stamler, J. S. *Nitric Oxide-Biol. Chem.* **1997**, *1*, 56−64.
(24) Carnahan, G. E.; Lenhert, P. G.; Ravichandran, R. *Acta Crystallogr.* **1978**, *B34*, 2645−2648.
(25) Cook, J. A.; Kim, S. Y.; Teague, D.; Krishna, M. C.; Pacelli, R.; Mitchell, J. B.; Vodovotz, Y.; Nims, R. W.; Christodoulou, D.; Miles, A. M.; Grisham, M. B.; Wink, D. A. *Anal. Biochem.* **1996**, *238*, 150−158.
(26) Alpert, C.; Ramdev, N.; George, D.; Loscalzo, J. *Anal. Biochem.* **1997**, *245*, 1−7.
(27) Samouilov, A.; Zweier, J. L. *Anal. Biochem.* **1998**, *258*, 322−330.
(28) Saville, B. *Analyst* **1958**, *83*, 670−672.
(29) Oae, S.; Shinhama, K.; Fujimori, K.; Kim, Y. H. *Bull. Chem. Soc. Jpn.* **1980**, *53*, 775−784.

Table 3. Comparison of RSNO Physical Parameters

	Ph_3CSNO[a]	SNAP[a]	SNAP[b]	*anti*-MeSNO[c]	*anti*-{MeSNO}$^-$ [c]
bond lengths, Å					
N−O	1.177(6)	1.206(3)	1.199(2)	1.1746	1.1950
S−N	1.792(5)	1.762(3)	1.763(2)	1.8653	2.4300
C−S	1.867(3)	1.842(2)	1.833(1)	1.8171	1.8265
bond angles, deg					
O−N−S	114.0(4)	114.9(2)	113.99(11)	116.7	118.3
N−S−C	102.1(2)	96.56(8)	100.80(7)	94.4	85.5
C−S−N−O dihedral angle	175.7	179.7	176.3	180[d]	180[d]
max dev from C−S−N−O plane, Å	0.0327	0.0024	0.028	0[d]	0[d]

[a] X-ray structure this study. [b] Reference 30. [c] Calculated by density functional theory B3LYP/6-311+G*. [d] Defined by C_s symmetry.

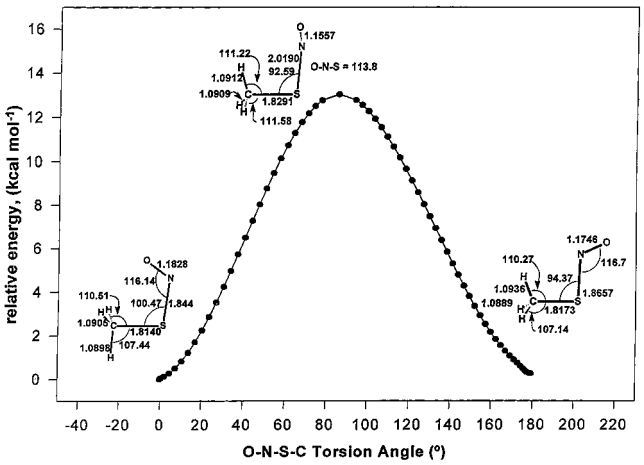

Figure 2. Transition-state configurations for the interconversion between syn and anti states for MeSNO.

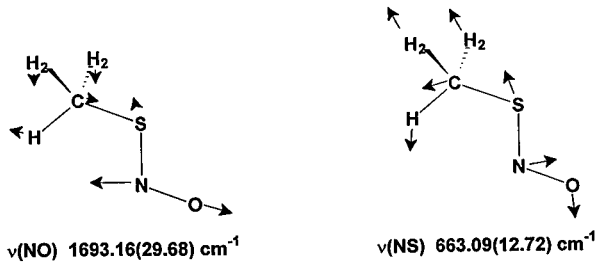

Figure 3. Theoretically predicted ^{15}N sensitive vibrational modes for MeSNO.

structural motif for the −S−N═O group. The ground-state geometry for MeSNO has two local minima, both with C_s symmetry. These are readily distinguished by their O−N−S−C dihedral angles, τ, and have been termed as syn with $\tau = 0°$ and anti with $\tau = 180°$. With density functional theory, B3LYP/6-311+G*, there is a very small energy difference, ~0.07 kcal/mol, in favor of the syn isomer. The ground-state geometries and the energy barrier for their interconversion are shown in Figure 2, which predicts a barrier of 12.86 kcal/mol for rotation around the O−N−S−C dihedral. Rotation around the bond leads to substantial weakening of the S−N bond length, and a contraction of both the N−O bond length and O−N−S bond angle to reach the transition state. Clearly this barrier suggests a significant S−NO delocalization, and the barrier depicted in Figure 2 most likely underestimates the experimental value. Further calculations for the reduced form of MeSNO show that the electron enters an S−N orbital with considerable antibonding character, and leads to a significant elongation of this bond (+0.56 Å). For the crystal structure of SNAP, and now that of Ph_3CSNO, only the anti conformation is observed. This could be due to steric effects for larger molecules, or the effect of solvation, since the calculations model MeSNO in the gas phase. It is unlikely that crystallization is kinetically controlled because only the anti conformation is observed for crystals of SNAP grown over a period of months, and therefore there is sufficient time to reach equilibrium and for the system to be under thermodynamic control. The crystallization of Ph_3CSNO from CH_2Cl_2 means there are no hydrogen bonding effects on crystal packing and, thus, there are unlikely to be any geometrical constraints upon the −S−N═O group. No evidence for anti/syn rotational isomers was observed in the solid state. In the published X-ray crystal structure of SNAP, crystal packing forces lead to a 6-fold disorder of the methyl group.[30]

We have reexamined structural details for SNAP with crystals grown in acetonitrile. The same geometric arrangement for the −SNO group, but a different overall conformation, was observed between the two structures. Structural details for the −SNO groups are summarized in Table 3. From acetonitrile SNAP crystallized in the space group $P2_12_12$, Table 1, which contained both the D and L isomers. The crystallographic asymmetric unit contains one of the two isomers, the other being related by inversion. Hydrogen bonding between the carboxylate hydrogen and the amide oxygen of a neighboring molecule ($H_{4a}-O_2$ 1.646 Å) and between the amide hydrogen and the carboxylate of a different molecule (N_2-O_{3b} 2.981 Å) is common to both crystal structures.[30] The main difference between the two structures appears to be based upon rotations along the $C_2(\alpha)-C_3(\beta)$ axis and the N_2-C_6 amide linkage. Consequent to the rotations, the acetyl methyl group is tilted away from the −SNO group and, unlike the reported structure, no disorder was observed for the protons of the methyl group in this conformation.

The crystal structure of Ph_3CSNO represents only the second small molecule high-resolution structure for the RSNO group, and these provide an interesting contrast, vide infra, with the recent structure of nitrosylated hemoglobin.[31]

Spectroscopic Characterization of RSNO. The use of a two-phase system for the preparation of *S*-nitrosothiols allowed for the ready incorporation of ^{15}N into compounds by using $Na^{15}NO_2$ as a starting reagent. Variable-temperature ^{15}N NMR spectra were acquired for $(CH_3)_3CS^{15}NO$ in d_8-toluene over the temperature range +65 to −81 °C, Figure 4. The results clearly demonstrate the dynamic behavior of $(CH_3)_3CSNO$ under these conditions and indicate that the complex is in the high-temperature regime at 20 °C. As the temperature is decreased the signal broadens and separates into two peaks, observed at −81 °C. The dynamic behavior observed is associated with syn−anti interconversion of RSNO via rotation around the S−N bond. It is possible to calculate the residence time, τ, from the frequency separation of the two peaks at the low-temperature limit, which, coupled with the coalescence temperature, can be

(30) Carnahan, G. E.; Lenhert, P. G.; Ravichandran, R. *Acta Crystallogr.* **1978**, *B34*, 2645−2648.
(31) Chan, N.-L.; Rogers, P. H.; Anone, A. *Biochemistry* **1998**, *37*, 16459−16464.

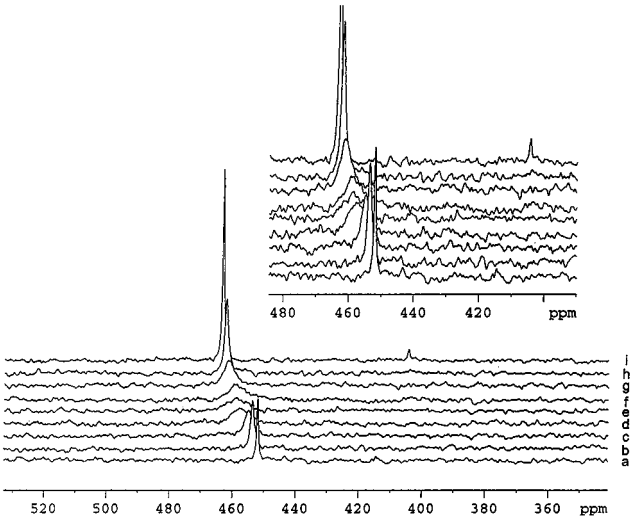

Figure 4. Variable-temperature ^{15}N NMR spectra for $(CH_3)_3CSNO$ at (a) +65, (b) +20, (c) +3, (d) −14, (e) −18, (f) −22, (g) −31, (h) −48, and (i) −81 °C.

used to calculate the rotational energy barrier for interconversion. The rotational barrier thus calculated for $(CH_3)_3CSNO$ is 10.7 ± 0.7 kcal/mol. This value is in very good agreement with that calculated by using density functional theory for MeSNO.

There is surprisingly little data available in the literature concerning the vibrational bands of the −SNO group[29,32] and these mainly focus on MeSNO.[33−35] Three compounds, GSNO, SNAP, Ph_3CSNO, and their −S^{15}NO-substituted analogues were prepared and the IR and Raman spectra were acquired. In addition, IR spectra were acquired for the parent thiol compounds, and the oxidized form of glutathione. The spectra presented in Figure 5 show the differences between the parent thiol and *S*-nitrosylated forms of glutathione. An important observation is the complete loss of the ν(S−H) stretch at ∼2600 cm^{-1} upon formation of the *S*-nitroso complex. This proves to be a sensitive marker for thiol contamination of an *S*-nitroso adduct. It was possible to observe this band for a 5% (w/w) thiol contamination of GSNO without saturating the transmittance for the GSNO modes. Determination of the vibrational signature from the −SNO group is not straightforward from the comparison of GSNO/GSH and SNAP/AP, which show a number of shifts and different bands. The spectra were obtained in the solid state and the shift in the bands is due, in part, to a disruption of the hydrogen-bonding network in the *S*-nitroso derivatives. This problem is not encountered for triphenylmethane thiol where no shifts and only two new bands were observed, at ∼1500 and ∼650 cm^{-1}. The assignment of these bands to the −SNO group was confirmed from the ^{15}N-labeled derivative, TPMT-S^{15}NO, and equivalent results were obtained for the normal and ^{15}N-labeled derivatives of GSNO and SNAP, Figure 6. The difference spectra for these complexes revealed isotope-sensitive vibrations at ∼1500 and ∼650 cm^{-1} for both Raman and infrared spectra; these results are summarized in Table 4. The bands correspond to the modes shown in Figure 2 and can be termed as ν_1(NO), ν_2(NS), and δ_3(ONS). Raman spectra were recorded with an excitation wavelength of 633 nm and so resonance enhancement was not expected. However, problems in spectral acquisition for solid Ph_3CSNO (visible λ_{max} 600 nm in CH_2Cl_2, ϵ_{600} 38.6 M^{-1} cm^{-1})[36] suggested that some laser-induced photodecomposition occurred. This is consistent with the observation that of the three RSNO species synthesized Ph_3CSNO is degraded the quickest by light. In the only previous report on the IR spectrum of Ph_3CSNO a broad band was reported between 1490 and 1530 cm^{-1} as being due to rotational isomers of the −SNO group.[32] No evidence for rotational isomers was observed in the crystal structure and the IR spectrum from dark green crystals of either the unlabeled or ^{15}N-labeled compounds showed only a single ν_1(NO) vibration.

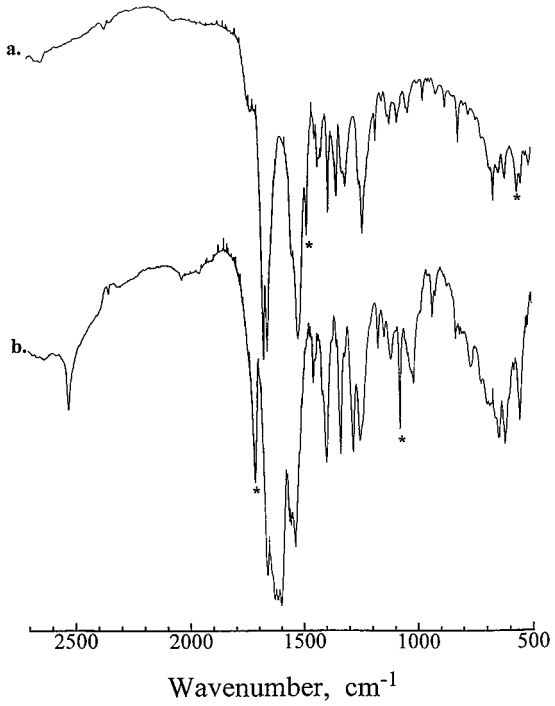

Figure 5. Identification of RSNO species by infrared spectroscopy: (a) GSNO and (b) GSH. The bands marked by an asterisk represent those readily identified as from one compound or another. The spectrum of GSSG (not shown) is readily distinguished from those above by the broad nature of the vibrations observed in the region 1750−100 cm^{-1}.

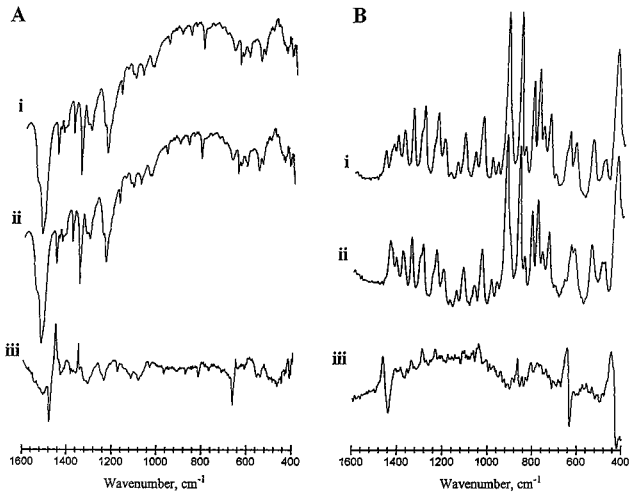

Figure 6. Vibrational bands of the −SNO group. The bands from the −SNO group are readily observed as derivative features in the difference spectrum between the unlabeled and ^{15}N isotopically labeled spectra: (A) IR and **(B)** Raman; (a) GSNO; (b) GS^{15}NO; and (c) difference spectrum.

(32) Kresze, G.; Uhlich, U. *Chem. Ber.* **1959**, *92*, 1048−1055.
(33) Byler, D. M.; Susi, H. *J. Mol. Struct.* **1981**, *77*, 25−36.
(34) Christensen, D. H.; Rastrup-Andersen, N.; Jones, D.; Klaboe, P.; Lippincott, E. R. S*pectrochim. Acta* **1968**, *24A*, 1581−11589.
(35) Mason, J. *J. Chem. Soc. A* **1969**, 1587−1592.

(36) For comparison: SNAP, ϵ_{600} 14.4 M^{-1} cm^{-1}; GSNO ϵ_{600} 1.3 M^{-1} cm^{-1}.

Table 4. Comparison of Vibrational Frequencies for RSNO Compounds

freq, cm^{-1} (^{15}N isotopic shift)	Ph_3CSNO^b		SNAP[b]		GSNO[b]		
	IR	Raman	IR	Raman	IR	Raman	MeSNO[a]
ν_1	1514(−23)	1513(−26)	1500(−24)	1500(−28)	1479(−23)	1467(−27)	1598.7(−29.5)
ν_2	650(−11)	678(−15)	670(−13)	672(−18)	664(−12)	647(−14)	625.9(−10.8)

[a] Calculated frequency. [b] KBr disk.

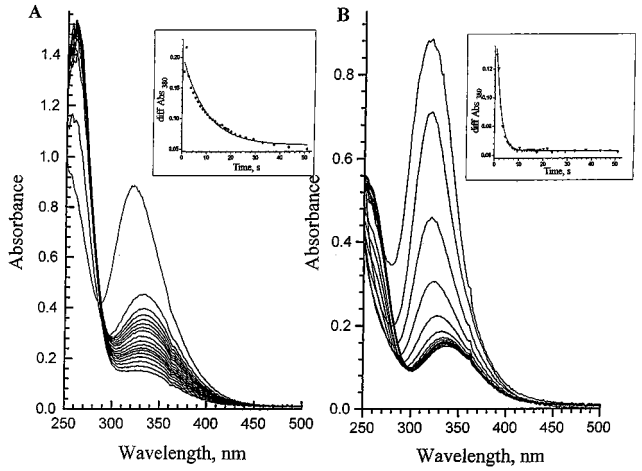

Figure 7. Reductive decomposition of RSNO in aqueous solutions under anaerobic conditions. (A) UV/vis spectra for the addition of 0.5 mM sodium dithionite to 1.5 mM GSNO. Inset: Time course for the reaction followed at 380 nm; the solid line represents a single-exponential fit to the data. (B) Addition of 0.15 mM dithionite to 0.5 mM SNAP. Inset: Time course for the reaction followed at 380 nm; the solid line represents a single-exponential fit to the data at this wavelength. Under these conditions the absorbance of sodium dithionite at 380 nm is negligible. Conditions: 50 mM Hepes, 100 mM NaCl, 500 μM EDTA, and pH 7.4

For a light-green precipitate of $Ph_3CS^{15}NO$ that had been exposed to light a new vibration was observed at 1455 cm^{-1}, which was due to photodecomposition.

Reductive Decomposition of RSNO Species. We investigated the possible redox mechanisms for the decomposition of the *S*-nitrosothiols GSNO, SNAP, and Ph_3CSNO in aqueous and organic solutions using cyclic voltammetry (CV), spectroelectrochemistry, and chemical methods. Initial attempts to follow the electrochemistry of GSNO in aqueous solutions by cyclic voltammetry indicated a possible reductive cleavage of GSNO. No current due to oxidation processes was observed, and processes due to reduction were near the onset of the solvent cutoff. The reduction of GSNO and subsequent generation of nitric oxide at these low potentials was verified by trapping with deoxymyoglobin and detecting the nitrosylmyoglobin formed by EPR. To pursue these investigations chemical methods were attempted to oxidize or reduce GSNO and SNAP. The addition of potassium ferricyanide to aqueous aerobic solutions of either of the compounds, GSNO or SNAP, produced no reaction demonstrating they were insensitive to oxidation based upon a simple electron-transfer mechanism at this potential.

In contrast to the stability of GSNO and SNAP toward oxidation both compounds were rapidly decomposed upon addition of dithionite under anaerobic conditions, Figure 7. An estimate of the half-lives for these reactions is 9.0 s for GSNO and 1.5 s for SNAP, based on a first-order fit at a single wavelength. By using the corresponding extinction coefficient it is possible to quantify the amount of RSNO lost upon addition of dithionite. These results show that the loss of RSNO by a net one-electron process is greater than that stoichiometrically required by the two-electron oxidation of dithionite. As outlined in the Experimental Section, there is an average of three equivalents of RSNO lost per dithionite, although the observed stoichiometry is highly variable and suggests the presence of several channels in the decomposition pathways. There was no indication of reversibility in this reaction when ferricyanide or oxygen was introduced to the sample following reduction by dithionite. No reaction was observed when ascorbate was used as a reductant indicating the reduction potential was less than 0 mV, which also excludes the possibility that the reaction is catalyzed by trace-metal contamination. In previous studies we have found an equimolar concentration of EDTA sufficient to quench copper-based decomposition of GSNO. Direct cyclic voltammetry of SNAP in CH_3CN gave a reduction potential of −1184 mV vs SCE.[37]

The solubility of Ph_3CSNO in organic solvents provides a larger window for electrochemistry, allowing cyclic voltammetry to be used. Direct CV was run in acetonitrile and methylene chloride solvents with similar results. In methylene chloride the CV of Ph_3CSNO shows a single reduction wave at −1360 mV, and no oxidation wave was observed when the sample was swept in a positive direction initially. The reduction wave was coupled to a number of product oxidation waves that are observed above 0 mV. The nature of the CV trace observed is dependent upon scan rate, which is indicative of the formation of short-lived reactive species. The major reduction product observed was the thiolate anion. This was verified by independent synthesis of the anion and analysis of its CV behavior in acetonitrile, the main feature being a large oxidation wave at +980 mV that is coupled to a much smaller reduction wave at −960 mV. From the CV scans it was not possible to obtain a clear product wave from $NO^{\bullet}$, the $NO^{\bullet/+}$ couple occurring at a similar potential to that observed for the thiolate anion. A combination of electrochemistry and UV/visible spectroscopy was used to clarify the reactions taking place, Figure 8. The species reduced at low potential is Ph_3CSNO, as shown by the decrease in absorption at 340 nm. Two products are observed spectroscopically with absorbances at 320 and 425 nm, which correspond to the thiolate (RS^-) and an unknown product. Both of these absorbances are lost as the potential is swept toward more oxidizing values. It has not been possible, yet, to identify the species giving rise to the absorbance at 420 nm. Two possibilities are a product with a nitrated or nitrosated phenyl ring, or a trityl species. The loss in this absorbance at 425 nm under subsequent oxidation conditions suggests it is unlikely to be from a nitrophenyl species. On the other hand the trityl radical, $Ph_3C^{\bullet}$, is known to be fairly stable and absorb at these wavelengths,[38] but a mechanism for its formation has not been determined. The two observed products have a different behavior over time and appear to form separately, the absorbance at 320 nm decays first but does not increase the absorbance at 420 nm.

Discussion

Although the *S*-nitrosothiol group can be generated relatively easily the physical characterization of this group has lagged

(37) Connelly, N. G.; Geiger, W. E. *Chem. Rev.* **1996**, *96*, 877−910.
(38) Sholle, V. D.; Rozantsev, E. G. *Russ. Chem. Rev.* **1973**, *42*, 1011−1020.

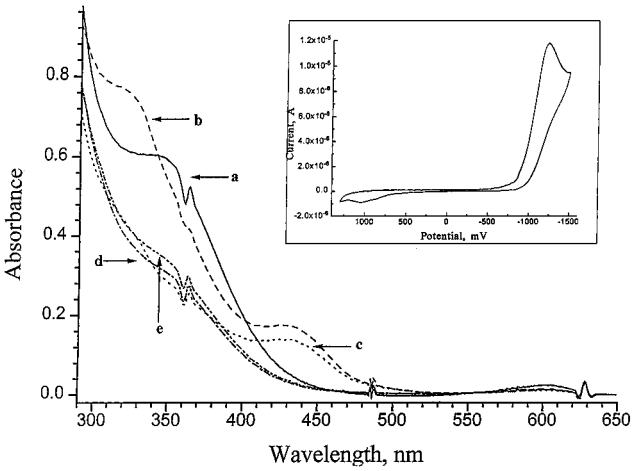

Figure 8. Spectroelectrochemistry for the reductive decomposition of Ph_3CSNO under anaerobic conditions. Absorption spectra showing the change in species observed with cycling the potential of the cell: (a) 0 mV, start; (b) −1300 mV; (c) 0 mV; (d) +1100 mV; and (e) 0 mV, stop. Inset: The CV for a diluted solution. Conditions: CH_2Cl_2 solvent + 0.1 M tetra-*n*-butylammonium hexafluorophosphate.

Table 5. Theoretical and Experimental Vibrational Frequencies (cm^{-1}) for Methylthionitrite Calculated by Density Functional Theory (B3LYP/6-311+G*)

exptl[a]	description	sym	MeSNO	^{15}N Shift[b]	$MeSNO^-$
	$\tau(CH_3)$	A″	131.9805	(−0.3065)	70.7501
	$\tau(CH_3)$	A′	225.6564	(0.1647)	136.4951 (A″)
250(−10)	δ(CSN)	A″	233.9891	(4.2220)	143.5358 (A′)
373(2)	δ(SNO)	A′	355.2371	(4.0113)	176.3028
646(13)	ν(SN)	A′	663.0910	(12.7217)	430.0316
735(1)	ν(SC)	A′	722.3850	(1.7555)	710.1410
977(4)	$\rho(CH_3)$	A′	973.5484	(−2.8062)	954.3580
948(1)	$\rho(CH_3)$	A″	990.9953	(−3.181)	961.0805
1304(1)	$\delta(CH_3)_{asym}$	A′	1356.4060	(−4.5058)	1344.2907
1433(−1)	$\delta(CH_3)_{sym}$	A″	1460.4647	(−5.44339)	1491.9197
1439(−1)	$\delta(CH_3)_{asym}$	A′	1485.4029	(−5.5394)	1496.7440
1535(28)	ν(NO)	A′	1693.1612	(29.6782)	1633.2716
2928(2)	ν(CH)	A′	3036.4533	(−11.5490)	2961.2042
	ν(CH)	A′	3121.8693	(−11.0762)	3016.2869
	ν(CH)	A″	3142.1250	(−11.0644)	3019.2601

[a] Taken from ref 29 with some bands not observed and observed ^{15}N isotopic shifts listed in brackets. [b] Calculated ^{15}N isotopic shifts with +ve to lower frequency.

someway behind studies on reactivity due to its inherent instability. The bond lengths and angles determined for Ph_3-CSNO and SNAP are very similar, with both compounds showing that the R−S−N−O linkage adopts an anti conformation with a formal S−N single bond and an N═O double bond and that the C−S−N−O framework is remarkably planar. Prior attempts to theoretically understand the structure and dynamics of *S*-nitrosothiols have largely been limited to calculations for methylthionitrite, CH_3SNO,[39,40] which has a well-understood gas-phase infrared spectrum[33,34] allowing a clear comparison between calculated and experimental vibrational modes, Table 5. Although the calculated and observed geometries for the CSNO framework are similar, and the relative observed/calculated isotope shifts from the SNO vibrations are closely matched, there are some significant differences between the theory and experiment. First, the experimental S−N bonds are ca. *0.1 Å shorter than calculated*, and second, the vibrational energies for the ν(NO) mode are about 150 cm^{-1} too *high in energy*. Thus, at the B3LYP/6-311+G* level of theory the degree of S−NO interaction is underestimated, and clearly some level of correlation is required to more closely match the experimental values. This is a widely recognized problem in calculations of sulfur oxides.[41] Nevertheless, the theoretical results illustrate how strongly delocalized and stabilizing the S−NO framework is, and in particular how large the energy barriers for rotation around the S−N bond must be. To date we are not aware of any data that deal with the energy barriers, or the spectroscopic characterization of the conformational dynamics of this group.

The variable-temperature ^{15}N NMR spectra that we have acquired shed light onto this problem, and clearly demonstrate the dynamic behavior of this class of compound. On the basis of a coalescence temperature of −18 °C and $\Delta\nu = 2393$ Hz,[42] the energy calculated for the rotational barrier, 10.7 kcal/mol, is considerable and is in good agreement with theoretical calculations. It is apparent, therefore, that rotation is hindered at room temperature, which is an important observation for the molecular modeling of Cys-SNO residues in proteins. The spectrum recorded at −81 °C represents the low-temperature limit for rotation, and the difference in signal intensity between the two peaks observed demonstrates that one conformation is highly favored. Because ^{15}N has a spin $I = {}^1/_2$, integration of these signals will provide their relative concentrations. However, reliable integration requires an exact knowledge of the relaxation properties, which are still under investigation. The observation of a favored conformation is in contrast with theoretical calculations for MeSNO that predict a small energy difference between conformers, which would result in approximately equal populations. The obvious difference in populations observed for $(CH_3)_3CSNO$ is, in part, based upon the steric influence of the *tert*-butyl group.

It is likely that conformational flexibility will influence compound stability as there is an increase in the S−N bond length at the transition state; elongation of this bond is also an initial step in the reductive release of nitric oxide from MeSNO (see later). These results support the previous calculations that report the thermal stability of RSNO was affected by the steric interactions involved in the dimerization to disulfide[43] and may also help to understand the different rates of trans nitrosylation observed. Calculations on the reduced form, $\{MeSNO\}^-$, indicate that the extra electron enters an S−N orbital with considerable antibonding character and leads to a significant elongation of this bond. This supports the experimental data that show reduction of RSNO rapidly leads to degradation of the compound under anaerobic conditions. It is important to build up structural data on the −SNO functional group, in part, to help model the Cys-SNO conformation in proteins more accurately, and to rationalize their reactivities.

In isolated solutions RSNO species are easily distinguished from the parent thiol by their color (pink to green), which is based upon an $n \rightarrow \pi^*$ charge-transfer absorption that is observed in the region 520−600 nm. Unfortunately this absorption is very weak ($\epsilon \sim 10$'s M^{-1} cm^{-1}) and is not readily observed for low concentrations of RSNO in multicomponent solutions. In addition, the broad nature of these absorbances can make differentiation between RSNO fragments problematic. Therefore, UV spectroscopy is not the technique best suited for the analysis of solutions of *S*-nitrosothiols. In our attempts to devise better methods of detection for these compounds we felt

(39) Bak, B.; Kristiansen, N. A. *J. Mol. Struct.* **1983**, *100*, 453−458.
(40) Schinke, R.; Hennig, S.; Untch, A.; Nonella, M.; Huber, J. R. *J. Chem. Phys.* **1989**, *91*, 2016−2029.
(41) Jensen, F. *J. Org. Chem.* **1992**, *57*, 6478.
(42) Sandstroem, J. *Dynamic NMR Spectroscopy*; Academic Press: New York, 1982.
(43) Bainbrigge, N.; Butler, A. R.; Gorbitz, C. H. *J. Chem Soc., Perkin Trans. 2* **1997**, 351−353.

that the vibrational signature of the *S*-nitrosothiol functional group was worth further examination. The IR data are limited to early reports on small molecules:[29,33,34] a single Raman spectra has been reported for MeSNO[34] and a different paper has demonstrated disulfide formation following exposure of metallothionein to nitric oxide, but not the modes from the −SNO group.[44] There have been many reports on factors affecting RSNO decomposition and although there is no definitive mechanism there is apparent agreement that the parent thiol helps to promote decomposition.[19] The current method for the determination of impurities in RSNO samples is by HPLC,[45−47] and as long as the RSNO sample is stable under the experimental conditions this proves to be an excellent technique for the determination of trace thiol and disulfide impurities. However, the failure to separate GSNO and GSH by preparative HPLC, despite their different retention times, suggests that a small amount of GSNO decomposes during HPLC analysis.[46] We have found that the loss of the ν(S−H) band at ∼2600 cm^{-1} following formation of the corresponding RSNO compound proves to be a sensitive marker of purity. Parent thiol contamination as low as 5 wt % could readily be detected in RSNO samples by quickly acquiring an IR spectrum. Previously it has been reported that GSNO can contain between 4% and 6% GSH.[45,46] It is true that this method is not suited as well to the determination of disulfide contamination; however, under general experimental conditions any disulfide present is generally stable and not readily reduced to the potentially active thiol or thiolate. There is no mention in the literature that disulfides affect the decomposition of *S*-nitrosothiols, nor have we found this to be the case.

The vibrational signature of the −SNO group was clearly distinguished by analyzing the normal and −S^{15}NO labeled compounds. The preparation of labeled compounds proves straightforward and relatively inexpensive, Na^{15}NO$_2$ being substituted for ordinary sodium nitrite. Two vibrations were observed at ∼1500 and ∼650 cm^{-1}, which correspond to the ν_1(NO) and ν_2(NS) stretching modes, respectively. The calculated frequency for the bending mode, δ_3(ONS), in MeSNO is 355 cm^{-1}, which lies below the window for KBr, and so this mode was not expected to be observed by IR for the other compounds. A ^{15}N-sensitive vibration was observed at 452 cm^{-1} in the Raman spectrum for GSNO, which could be attributed to this vibrational mode. We are currently investigating whether it is possible to detect these isotope-sensitive −SNO vibrations in proteins. The broad vibrational envelope for these very large molecules often makes it hard to distinguish individual bands. Therefore, it would be beneficial to enhance the signal from the mode of interest, as observed in resonance Raman spectroscopy. Preliminary results with Ph$_3$CSNO are not encouraging as the partial overlap of the absorption envelope and laser excitation led to laser-induced photodecomposition of the product. Thus, it may prove difficult to increase the sensitivity of this technique for the detection of −SNO by using resonance enhanced Raman spectroscopy. This is also suggested, somewhat obliquely, by photochemical studies of the decomposition of *S*-nitrosothiols.[48]

Among the factors that can affect the decomposition of *S*-nitrosothiols are trace metal contamination (copper or mercury), other thiols, and light. It is possible to propose competing pathways for decomposition, shown in eqs 1 and 2, with the route chosen dependent upon solution composition. Metal-based decomposition can also promote loss of NO$^\bullet$ via a nonhydrolytic pathway.[49] The conversion of NO$^\bullet$ to nitrite (as detected by the Saville assay) will be enhanced at low pH and high NO$^\bullet$ concentrations.

homolytic

$$\mathrm{RSNO} \xrightarrow{h\nu} \mathrm{RS}^\bullet + \mathrm{NO}^\bullet \xrightarrow{\mathrm{RSNO}} \mathrm{RSSR} + 2\mathrm{NO}^\bullet \qquad (1)$$

hydrolysis

$$\mathrm{RSNO} + \mathrm{H_2O} \xrightarrow{\mathrm{M}^{n+}} \mathrm{RSH} + \mathrm{NO_2}^- + \mathrm{H}^+ \qquad (2)$$

It is not surprising, then, that there is some confusion in this area. Even the Saville reaction has not been characterized in terms of intermediates. Moreover, the overall method calls for an excess of mercury that putatively acts as a catalyst for decomposition.

The aim of this paper is not to present a definitive mechanism of decomposition but to explore another set of important factors, the interaction with oxidants and reductants. The results obtained clearly show that the RSNO group is stable to oxidation. This is not surprising, as a facile decomposition pathway is not obvious. Conversely it was found that following reduction *S*-nitrosothiols rapidly decomposed. It is easy to visualize a mechanism for this reaction.

reduction

$$\mathrm{RSNO} + \mathrm{e}^- \rightarrow \{\mathrm{RSNO}\}^{\bullet -} \rightarrow \mathrm{RS}^- + \mathrm{NO}^\bullet \qquad (3)$$

This reaction is similar to the proposed reduction of GSNO by superoxide to give nitric oxide, thiolate anion, and dioxygen.[50] However, both of these are the opposite of the mechanism described by Gow et al.,[13,51] although neither is the microscopic reverse. They propose *S*-nitrosothiol formation can occur from the direct reaction between a thiol and nitric oxide prior to the interaction with an electron acceptor. It is important, therefore, to determine the conditions under which the forward and reverse directions of this reaction will be favored. In their work Gow et al. used aerobic solutions in which oxygen acted as the electron acceptor to generate superoxide. The conditions involved relatively high concentrations of the electron acceptor and of the thiol and very low concentration of nitric oxide for *S*-nitrosothiol formation. From the results we have obtained using dithionite as a reductant it is clear that in the absence of a suitable electron acceptor the proposed intermediate, {RSNO}$^{\bullet -}$, is unstable decomposing to nitric oxide and thiolate. This is supported by the fast rate of decomposition and suggests the overall balance of products, *S*-nitrosothiol or thiolate and nitric oxide, will be determined by the availability of the electron donor or acceptor. What then is the fate of *S*-nitrosothiols in physiological systems? The reduction mechanism for the decomposition for this class of compound may represent a new pathway to the selective delivery of nitric oxide in physiological systems, which would be based on a simple electron donor or a reductase enzyme. This would, perhaps, be a better pathway

(44) Kroncke, K. D.; Fehsel, K.; Schmidt, T.; Zenke, F. T.; Dasting, I.; Wesener, J. R.; Bettermann, H.; Breunig, K. D.; Kolb-Bachofen, V. *Biochem. Biophys. Res. Commun.* **1994**, *200*, 1105−1110.

(45) Becker, K.; Gui, M.; Schirmer, R. H. *Eur. J. Biochem.* **1995**, *234*, 472−478.

(46) Gorren, A. C. F.; Schrammel, A.; Schmidt, K.; Mayer, B. *Arch. Biochem. Biophys.* **1996**, *330*, 219−228.

(47) Welch, G. N.; Upchurch, G. R.; Loscalzo, J. *Methods Enzymol.* **1996**, *268*, 293−298.

(48) Mohney, B. K.; Wang, C.; Walker, G. C. *Biophys. J.* **1998**, *74*, A144.

(49) Williams, D. L. H. *Transition Met. Chem.* **1996**, *21*, 189−191.

(50) Trujillo, M.; Alvarez, M. N.; Peluffo, G.; Freeman, B. A.; Radi, R. *J. Biol. Chem.* **1998**, *273*, 7828−7834.

(51) Gow, A. J.; Buerk, D. G.; Ischiropoulos, H. *J. Biol. Chem.* **1997**, *272*, 2841−2845.

for the release of nitric oxide from *S*-nitrosothiols in physiological systems as it does not lead to thiyl radical or nitrite formation. Obviously this hypothetical route for the delivery of nitric oxide requires further investigation, as does the whole area of the physiological role of *S*-nitrosothiols.

Taken together these results have important implications for understanding the bonding and reactivity of nitrosylated cysteine residues in proteins.[31] Clearly the thermodynamically preferred conformation for these groups will be rigidly planar with the anti conformation favored. In this study the difference in ground-state energy between syn and anti conformations appears to be a function of the specific steric constraints for the moiety. There is however a substantial barrier for interconversion of these conformers, and twisting or any disruption of the planarity of this group destabilizes the fragment toward S−N homolysis and release of NO. We note that in the recent structure of β_{93}-SNOHbNO, nitrosylation of the β-cysteine$_{93}$ residue results in a marked change in the tertiary structure of the carboxylate terminal of this subunit. Remarkably, among the changes found is the rotation of the SNO group such that the C−S−N−O torsion angle is 87°, that is it is near the maximum for the conformational curve shown in Figure 2. Thus the β_{93}-SNO group is destabilized by ca. 10 kcal/mol in this conformation, and suggests that this fragment is relatively close to the transition state for S−N homolysis or reductive cleavage. It is quite possible that RSNO conformational dynamics may play a role in NO release from Cys$_{\beta 93}$ in hemoglobin upon R to T transformation.[52]

Conclusions

A new method for the formation of small molecule *S*-nitrosothiols has been developed on the basis of a two-phase aqueous−organic solution system. As part of this work crystals of *S*-nitrosotriphenylmethanethiol were prepared and structural details were obtained from X-ray crystallography. This structure bears close similarity to the previously determined structure for SNAP, and the theoretically predicted ground state for MeSNO. The R−S−N═O group adopts an anti conformation with bond lengths indicating an S−N single bond and an N═O double bond. Analysis of a group of RSNO compounds by vibrational spectroscopy showed that this was an effective method for the identification of the −SNO functional group. The use of ^{15}N isotope labeling confirmed that vibrational bands at ∼1500 and ∼650 cm^{-1} were based on the −SNO group. Alternative patterns of decomposition for *S*-nitrosothiols have been investigated by using chemical and electrochemical methods of oxidation and reduction. It was observed that the RSNO group rapidly decomposes following reduction. This may represent a selective pathway for the delivery of nitric oxide in physiological systems from *S*-nitrosothiols. Finally, these results suggest that nitrosylation of the hemoglobin results in a markedly destabilized β_{93}-SNO group that will either be readily reductively or homolytically cleaved.

Materials and Methods

Preparation of Compounds. The *S*-nitroso adducts of glutathione and D,L-acetylpenicillamine were prepared as reported in the literature.[13,51,53,54] An alternative method of preparation was also developed for SNAP. This consisted of bubbling NO gas through a solution of d,L-acetylpenicillamine in methanol for 3 h. A green color developed that darkened with prolonged bubbling. The solution was diluted with CH_2Cl_2 and platelet-like crystals that were green with red reflections were recovered at −10 °C after 4 days. As reported previously the DSC of GSNO and SNAP showed these compounds decomposed endothermically at 150 °C.[43] We observed a second, larger, endothermic process at 202 °C. Dark-green crystals of SNAP were prepared by slow crystallization at −10 °C in acetonitrile.

S-Nitrosotriphenylmethanethiol, Ph_3CSNO, was prepared as follows: In a two-phase reaction triphenylmethanethiol (0.5 mol/5 mL of CH_2Cl_2) was shaken with an acidified solution of sodium nitrite (1 mol of $NaNO_2$ in 4 mL of 0.1 M HCl). A green color rapidly formed. The solution was allowed to stand, the clear aqueous phase was then removed, and cold methanol (20 mL) was added. Formation of green crystals occurred over a matter of hours at −10 °C. These were removed and dried under vacuum. Microanalysis (%) found the following (theory): Ph_3CSNO: C, 74.17 (74.72); H, 5.03 (4.95); N, 4.46 (4.59). In contrast to GSNO and SNAP the DSC of Ph_3CSNO showed a single exothermic process at 110 °C for compound degradation.

S-Nitroso-2-methylpropanethiol, $(CH_3)_3CS^{15}NO$, was prepared in an analogous manner to Ph_3CSNO. The free thiol was diluted in d_8-toluene (20 μL/600 μL) and an aqueous solution of $Na^{15}NO_2$ added (800 mM/300 μL). The reaction started following the addition of HCl (6 M/100 μL) and shaking. The aqueous layer was removed. The organic layer was shaken with a further aliquot of water and then eluted from a short alumina column. The resulting dark green solution recovered was used in the subsequent NMR experiments.

The thiolate salt of triphenylmethanethiol was prepared by stirring a solution of the thiol with sodium metal in benzene under anaerobic conditions. A fine white precipitate of the thiolate was recovered by filtration after 2 days.

All materials were purchased from Sigma-Aldrich, except where noted otherwise, and were ACS grade or higher. Where isotopically labeled products were required, $Na^{15}NO_2$ (Cambridge Isotopes) was used. Millipore water was used in all aqueous preparations. Analytical data on the compounds were obtained from Atlantic Microlab Inc.

Chemical Reduction Reactivity. In an inert atmosphere box maintained at low partial pressures of oxygen with a circulating scrubber stock solutions of *S*-nitrosothiols and reductants were prepared with use of oxygen-free buffers. The *S*-nitrosothiol solution is diluted to the desired concentration, 0.5−2 mM, from a 20 mM stock solution, in a 3 mL cuvette containing a magnetic stirrer bar. The concentration is determined by using the extinction coefficient for the *S*-nitrosothiol. An aliquot of dithionite was then added, final concentration 0.15−0.5 mM, and the kinetics of *S*-nitrosothiol decomposition was followed spectrophotometrically. The ratio A_{335}/A_{315} was used to check that all the dithionite was consumed during the reaction, and final RSNO concentrations were determined by using the extinction coefficient at 380 nm for these. The product/reactant stoichiometry is 3.1 ± 0.3 ($n = 4$) on the basis of these criteria. In the case of ascorbate there was no reaction of 5 mM ascorbate with 1 mM GSNO at pH 7.0.

X-ray Crystallography. Structural data were collected on a Siemens P4 diffractometer equipped with a molybdenum tube [$\lambda(K\alpha_1) = 0.70926$ Å] and a graphite monochromator at 25 °C. Crystal data and refinement parameters for both structures are given in Table 1. Three standard reflections were measured after every 97 reflections and exhibited no significant loss in intensity.

(a) Ph_3CSNO. For a green crystal of *S*-nitrosotriphenylmethanethiol a total of 1724 ($R_{int} = 0.0216$) independent reflections were gathered in the 2θ range of 5.56−50°. The data were not corrected for absorption. The compound crystallized in the orthorhombic space group $Pna2_1$ ($Z = 4$) and the structure was solved by direct methods and refined by least-squares and a full-matrix least-squares process on F^2 by using structure solution programs from the SHELXTL system.[55] All non-hydrogen atoms were refined anisotropically whereas the hydrogen atoms were located in successive Fourier maps and refined isotropically. The final refinement parameters were $R_1 = 0.0415$ and $wR_2 = 0.1143$ for data with $F > 4\sigma(F)$ ($R_1 = 0.0446$ and $wR_2 = 0.1219$ for all data

(52) Stamler, J. S.; Jia, L.; Eu, J. P.; McMahon, T. J.; Demchenko, I. T.; Bonaventura, J.; Gernert, K.; Piantadosi, C. A. *Science* **1997**, *276*, 2034−2037.

(53) Hart, T. W. *Tetrahedron Lett.* **1985**, *26*, 2013.

(54) Field, L.; Dilts, R. V.; Ravichandran, R.; Lenhert, P. G.; Carnahan, G. E. *J. Chem. Soc., Chem. Commun.* **1978**, 249−250.

(55) Sheldrik, G. M.; 5.03/Iris ed.; Sheldrik, G. M., Ed.; Siemens Analytical X-ray instruments: Madison WI, 1995.

giving a data to parameter ration of 6.6:1). The maximum and minimum residual intensities were 0.203and -0.285 eÅ^{-3}, respectively.

(b) SNAP. A dark-green crystal with red reflections of *S*-nitroso-acetylpenicillamine was selected for structure analysis. A total of 1409 ($R_{int} = 0.0171$) independent reflections were gathered in the 2θ range of 5.5−50°. The data were not corrected for absorption. The compound crystallized in the orthorhombic space group $P2_12_12$ ($Z = 4$) and the structure was solved by direct methods and refined by least-squares and a full-matrix least-squares process on F^2 by using structure solution programs from the SHELXTL system.[55] All non-hydrogen atoms were refined anisotropically whereas the hydrogen atoms were located in successive Fourier maps and refined isotropically. The final refinement parameters were $R_1 = 0.0256$ and $wR_2 = 0.0677$ for data with $F > 4\sigma(F)$ ($R_1 = 0.0289$ and $wR_2 = 0.0795$ for all data giving a data to parameter ration of 8.0:1). The maximum and minimum residual intensities were 0.144 and -0.205 eÅ^{-3}, respectively.

NMR Spectroscopy. NMR spectra were acquired on a Bruker Advance-400 spectrometer operating at 40.55 MHz for ^{15}N. The sample was equilibrated for 10 min at each temperature prior to data collection, 256 transients were acquired with a 60° pulse, 2.0 s acquisition time, and 3.5 s delay time. The data were multiplied by an exponential window function with a 25 Hz line broadening factor prior to Fourier transformation. Spectra were referenced to an external standard of $Na^{15}NO_2$ at 0 ppm.[56] Temperature corrections were applied to experimental values based upon a calibration of thermocouple performance against a methanol/ethylene glycol standard.

Raman Spectroscopy. A Solution 633 Raman Laser System (Detection Limit Technology) was used to acquire spectra for solid samples of GSNO and SNAP and for a solution of Ph_3CSNO in CH_2Cl_2. It was necessary to dissolve Ph_3CSNO due to laser-induced photodecomposition of the solid, and the laser used had an excitation wavelength of 633 nm.

Infrared Spectroscopy. Spectra were acquired with use of a MIDAC FTIR spectrophotometer, recording 32 transients at a resolution of 1 cm^{-1}. Solid spectra were obtained as KBr pellets or as a mull in a fluorocarbon polymer between KBr plates. Solution spectra were recorded by using CH_2Cl_2 as a solvent.

Electrochemistry. Cyclic voltammetry experiments were conducted by using a BAS50w potentiostat (Bioanalytical Sciences) with a platinum wire auxiliary electrode, a platinum working electrode, and a silver reference electrode. Experiments were performed anaerobically in a Vacuum atmospheres Inert Atmosphere box. Spectroelectrochemistry investigations were performed by using an optical cell in which a platinum gauze working electrode was sandwiched between two quartz windows. Anaerobic, dry, solvents were used and the sample purged with argon during the experiment. Absorption spectra were acquired on a Hewlett-Packard HP8453 diode array spectrophotometer. In both sets of experiments 0.1 M tetra-*n*-butylammonium hexafluorophosphate was used as an electrolyte and ferrocene was added as an internal standard.[37,57]

(56) There remains some confusion in the literature over the appropriate reference sample and chemical shift scale to use in nitrogen NMR spectroscopy.[11,62,63] In our experiments nitromethane was used as an external reference at 0 ppm and signals observed at lower field assigned positive chemical shifts. Thus, on this scale, $MeNO_2$ δ 0.0 ppm, KNO_3 (1 M, D_2O, pD 8) δ −3.5 ppm, $NaNO_2$ (1 M, D_2O, pD 9.4) δ 232.0 ppm, $(CH_3)_3CSNO$ (0.25 M, d_8-toluene) δ 453.5 ppm.

UV/Visible Spectroscopy. Absorption spectra were acquired on a Hewlett-Packard HP8453 diode array spectrophotometer. For studies on aqueous systems in anaerobic environments fiber-optic cables were used to record the spectra in an inert-atmosphere box (Belle Technology).

Theoretical Calculations. The calculations described here were performed by using Gaussian94[58] implemented on a Silicon Graphics Iris Indigo workstation. Full optimizations were performed initially at the restricted Hartree−Fock (HF) level by using the polarized split valence 6-31G* basis sets before the final optimizations which were performed by density functional theory with use of Becke's 3 parameter functional[59] and double-ζ sets, 6-311+G*. It has recently been shown that related nitrogen oxide anions exhibit Hartree−Fock instability and that an effective method to model this is with Becke's three-parameter hybrid functions.[60] After determination of the ground-state geometries for the syn and anti conformations of methylthionitrite the transition state for their conversion was determined by using the synchronous transit-guided quasi-Newton algorithm developed by Schlegel et al.[61] The optimized transition states were tested by stepping through the internal reaction coordinate to verify that the saddle separated the minima described by the anti and syn structures. The reduced geometry for methylthionitrite was calculated for the anti geometry and gave a ground state with the structure that corresponds to a local minimal geometry, as gauged for its frequencies.

Acknowledgment. This work was made possible by support from the NIH, grant GM-53828, and a Teacher-Scholar award from the Henry and Camille Dreyfus Foundation. We thank Prof. K. C. Carron for the use of his Raman equipment and assistance in its operation.

JA9901314

(57) Formal potentials for the ferrocene$^{+1/0}$ couple vs SCE: +400 mV, CH_3CN solvent; +460 mV, CH_2Cl_2 solvent.

(58) Frisch, M. J.; Trucks, G. W.; Schlegel, H. B.; Gill, P. M. W.; Johnson, B. G.; Robb, M. A.; Cheeseman, J. R.; Keith, T.; Petersson, G. A.; Montgomery, J. A.; Raghavachari, K.; Al-Laham, M. A.; Zakrzewski, V. G.; Ortiz, J. V.; Foresman, J. B.; Cioslowski, J.; Stefanov, B. B.; Nanayakkara, A.; Challacombe, M.; Peng, C. Y.; Ayala, P. Y.; Chen, W.; Wong, M. W.; Andres, J. L.; Replogle, E. S.; Gomperts, R.; Martin, R. L.; Fox, D. J.; Binkley, J. S.; Defrees, D. J.; Baker, J.; Stewart, J. P.; Head-Gordon, M.; Gonzalez, C.; Pople, J. A.; Frisch, M. J.; Trucks, G. W.; Schlegel, H. B.; Gill, P. M. W.; Johnson, B. G.; Robb, M. A.; Cheeseman, J. R.; Keith, T.; Petersson, G. A.; Montgomery, J. A.; Raghavachari, K.; Al-Laham, M. A.; Zakrzewski, V. G.; Ortiz, J. V.; Foresman, J. B.; Cioslowski, J.; Stefanov, B. B.; Nanayakkara, A.; Challacombe, M.; Peng, C. Y.; Ayala, P. Y.; Chen, W.; Wong, M. W.; Andres, J. L.; Replogle, E. S.; Gomperts, R.; Martin, R. L.; Fox, D. J.; Binkley, J. S.; Defrees, D. J.; Baker, J.; Stewart, J. P.; Head-Gordon, M.; Gonzalez, C.; Pople, J. A., Eds.; Gaussian, Inc.: Pittsburgh, PA, 1995.

(59) Becke, A. D. *J. Chem. Phys.* **1993**, *98*, 5648−5652.

(60) Tsai, H.-H.; Hamilton, T. P.; Tsai, J.-H. M.; Harrison, J. G.; Beckman, J. S. *J. Phys. Chem.* **1996**, *100*, 6942−6949.

(61) Peng, C.; Schlegel, H. B. *Isr. J. Chem.* **1993**, *33*, 449−54.

(62) Witanowski, M.; Stefaniak, L.; Webb, G. A. *Annu. Rep. NMR Spectrosc.* **1993**, *25*, 1−480.

(63) Mason, J. In *Multinuclear NMR*; Mason, J., Ed.; Plenum Press: New York, 1987; pp 335−368.